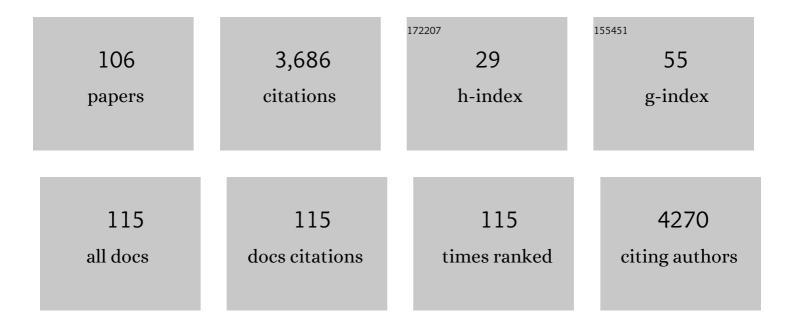
Vicente Grau

List of Publications by Year in descending order

Source: https://exaly.com/author-pdf/1504076/publications.pdf Version: 2024-02-01



VICENTE CDALL

#	Article	IF	CITATIONS
1	Understanding and Improving Risk Assessment After Myocardial Infarction Using Automated Left Ventricular ShapeÂAnalysis. JACC: Cardiovascular Imaging, 2022, 15, 1563-1574.	2.3	21
2	Predicting 3D Cardiac Deformations withÂPoint Cloud Autoencoders. Lecture Notes in Computer Science, 2022, , 219-228.	1.0	7
3	A Multi-view Crossover Attention U-Net Cascade withÂFourier Domain Adaptation forÂMulti-domain Cardiac MRI Segmentation. Lecture Notes in Computer Science, 2022, , 323-334.	1.0	2
4	Generating Subpopulation-Specific Biventricular Anatomy Models Using Conditional Point Cloud Variational Autoencoders. Lecture Notes in Computer Science, 2022, , 75-83.	1.0	9
5	A deep learning pipeline to simulate fluorodeoxyglucose (FDG) uptake in head and neck cancers using non-contrast CT images without the administration of radioactive tracer. Insights Into Imaging, 2022, 13, 45.	1.6	2
6	Semi-Supervised Coronary Vessels Segmentation from Invasive Coronary Angiography with Connectivity-Preserving Loss Function. , 2022, , .		1
7	Generation of 12-Lead Electrocardiogram with Subject-Specific, Image-Derived Characteristics Using a Conditional Variational Autoencoder. , 2022, , .		2
8	Combined Generation of Electrocardiogram and Cardiac Anatomy Models Using Multi-Modal Variational Autoencoders. , 2022, , .		11
9	Optimised Misalignment Correction from Cine MR Slices Using Statistical Shape Model. Lecture Notes in Computer Science, 2021, , 201-209.	1.0	4
10	Biventricular Surface Reconstruction From Cine Mri Contours Using Point Completion Networks. , 2021, , .		17
11	Left Ventricle Quantification Challenge: A Comprehensive Comparison and Evaluation of Segmentation and Regression for Mid-Ventricular Short-Axis Cardiac MR Data. IEEE Journal of Biomedical and Health Informatics, 2021, 25, 3541-3553.	3.9	8
12	Inference of ventricular activation properties from non-invasive electrocardiography. Medical Image Analysis, 2021, 73, 102143.	7.0	19
13	A completely automated pipeline for 3D reconstruction of human heart from 2D cine magnetic resonance slices. Philosophical Transactions Series A, Mathematical, Physical, and Engineering Sciences, 2021, 379, 20200257.	1.6	22
14	Emerging artificial intelligence applications in liver magnetic resonance imaging. World Journal of Gastroenterology, 2021, 27, 6825-6843.	1.4	5
15	Inference of Ventricular Activation Properties from Twelve-lead Electrocardiogram. , 2021, , .		0
16	Point-Cloud Method for Automated 3D Coronary Tree Reconstruction From Multiple Non-Simultaneous Angiographic Projections. IEEE Transactions on Medical Imaging, 2020, 39, 1278-1290.	5.4	14
17	The â€~Digital Twin' to enable the vision of precision cardiology. European Heart Journal, 2020, 41, 4556-4564.	1.0	319
18	A Deep Learning Pipeline to Automate High-Resolution Arterial Segmentation with or without Intravenous Contrast. Annals of Surgery, 2020, Publish Ahead of Print, .	2.1	9

#	Article	IF	CITATIONS
19	MRI-Based Computational Torso/Biventricular Multiscale Models to Investigate the Impact of Anatomical Variability on the ECG QRS Complex. Frontiers in Physiology, 2019, 10, 1103.	1.3	35
20	Ventricle Surface Reconstruction from Cardiac MR Slices Using Deep Learning. Lecture Notes in Computer Science, 2019, , 342-351.	1.0	7
21	Patch-based lung ventilation estimation using multi-layer supervoxels. Computerized Medical Imaging and Graphics, 2019, 74, 49-60.	3.5	5
22	ISACHI: Integrated Segmentation and Alignment Correction for Heart Images. Lecture Notes in Computer Science, 2019, , 171-180.	1.0	1
23	Automated localization and quality control of the aorta in cine CMR can significantly accelerate processing of the UK Biobank population data. PLoS ONE, 2019, 14, e0212272.	1.1	26
24	Classification of amyloid PET images using novel features for early diagnosis of Alzheimer's disease and mild cognitive impairment conversion. Nuclear Medicine Communications, 2019, 40, 242-248.	0.5	19
25	Segmentation of Vasculature From Fluorescently Labeled Endothelial Cells in Multi-Photon Microscopy Images. IEEE Transactions on Medical Imaging, 2019, 38, 1-10.	5.4	22
26	Automated Motion Correction and 3D Vessel Centerlines Reconstruction from Non-simultaneous Angiographic Projections. Lecture Notes in Computer Science, 2019, , 12-20.	1.0	3
27	Optimized Rigid Motion Correction from Multiple Non-simultaneous X-Ray Angiographic Projections. Lecture Notes in Computer Science, 2019, , 61-69.	1.0	1
28	Statistical Shape Modeling of the Left Ventricle: Myocardial Infarct Classification Challenge. IEEE Journal of Biomedical and Health Informatics, 2018, 22, 503-515.	3.9	61
29	Electrocardiogram phenotypes in hypertrophic cardiomyopathy caused by distinct mechanisms: apico-basal repolarization gradients vs. Purkinje-myocardial coupling abnormalities. Europace, 2018, 20, iii102-iii112.	0.7	29
30	Surface Mesh Reconstruction from Cardiac MRI Contours. Journal of Imaging, 2018, 4, 16.	1.7	16
31	Super Resolution of Cardiac Cine MRI Sequences Using Deep Learning. Lecture Notes in Computer Science, 2018, , 23-31.	1.0	12
32	3D reconstruction of coronary arteries from 2D angiographic projections using non-uniform rational basis splines (NURBS) for accurate modelling of coronary stenoses. PLoS ONE, 2018, 13, e0190650.	1.1	32
33	XeMRI to CT Lung Image Registration Enhanced with Personalized 4DCT-Derived Motion Model. Lecture Notes in Computer Science, 2018, , 260-271.	1.0	0
34	Regional lung ventilation estimation based on supervoxel tracking. , 2018, , .		1
35	Left-Ventricle Basal Region Constrained Parametric Mapping to Unitary Domain. Lecture Notes in Computer Science, 2017, , 163-171.	1.0	0
36	Transformation diffusion reconstruction of three-dimensional histology volumes from two-dimensional image stacks. Medical Image Analysis, 2017, 38, 184-204.	7.0	15

#	Article	IF	CITATIONS
37	Monte Carlo Simulations of Diffusion Weighted MRI in Myocardium: Validation and Sensitivity Analysis. IEEE Transactions on Medical Imaging, 2017, 36, 1316-1325.	5.4	15
38	Non-local Graph-Based Regularization forÂDeformable Image Registration. Lecture Notes in Computer Science, 2017, , 199-207.	1.0	2
39	Evaluation of nonâ€Gaussian diffusion in cardiac MRI. Magnetic Resonance in Medicine, 2017, 78, 1174-1186.	1.9	12
40	Chronic Obstructive Pulmonary Disease: Lobar Analysis with Hyperpolarized ¹²⁹ Xe MR Imaging. Radiology, 2017, 282, 857-868.	3.6	41
41	Cardiac Mesh Reconstruction from Sparse, Heterogeneous Contours. Communications in Computer and Information Science, 2017, , 169-181.	0.4	2
42	Automated LGE Myocardial Scar Segmentation Using MaskSLIC Supervoxels - Replicating the Clinical Method. Communications in Computer and Information Science, 2017, , 229-236.	0.4	1
43	MRI-Based Heart and Torso Personalization for Computer Modeling and Simulation of Cardiac Electrophysiology. Lecture Notes in Computer Science, 2017, , 61-70.	1.0	4
44	Supervoxels for graph cuts-based deformable image registration using guided image filtering. Journal of Electronic Imaging, 2017, 26, 1.	0.5	8
45	Reconstruction of 3D Cardiac MR Images fromÂ2D Slices Using Directional Total Variation. Lecture Notes in Computer Science, 2017, , 127-135.	1.0	4
46	Graph Cuts-Based Registration Revisited: A Novel Approach for Lung Image Registration Using Supervoxels and Image-Guided Filtering. , 2016, , .		4
47	A poroelastic model coupled to a fluid network with applications in lung modelling. International Journal for Numerical Methods in Biomedical Engineering, 2016, 32, e02731.	1.0	39
48	Prospective acceleration of diffusion tensor imaging with compressed sensing using adaptive dictionaries. Magnetic Resonance in Medicine, 2016, 76, 248-258.	1.9	22
49	Anomalous Diffusion in Cardiac Tissue as an Index of Myocardial Microstructure. IEEE Transactions on Medical Imaging, 2016, 35, 2200-2207.	5.4	28
50	Development of Real-Time Magnetic Resonance Imaging of Mouse Hearts at 9.4 Tesla— Simulations and First Application. IEEE Transactions on Medical Imaging, 2016, 35, 912-920.	5.4	10
51	Myocardial Infarction Detection from Left Ventricular Shapes Using a Random Forest. Lecture Notes in Computer Science, 2016, , 180-189.	1.0	3
52	Orientation-Sensitive Overlap Measures forÂtheÂValidation of Medical Image Segmentations. Lecture Notes in Computer Science, 2016, , 361-369.	1.0	0
53	Dynamic flow characteristics in normal and asthmatic lungs. International Journal for Numerical Methods in Biomedical Engineering, 2015, 31, .	1.0	26
54	Optimized radiofrequency coil setup for MR examination of living isolated rat hearts in a horizontal 9.4T magnet. Magnetic Resonance in Medicine, 2015, 73, 2398-2405.	1.9	3

#	Article	IF	CITATIONS
55	Review of automatic pulmonary lobe segmentation methods from CT. Computerized Medical Imaging and Graphics, 2015, 40, 13-29.	3.5	51
56	Fuzzy Segmentation of the Left Ventricle in Cardiac MRI Using Physiological Constraints. Lecture Notes in Computer Science, 2015, , 231-239.	1.0	0
57	Quantitative Study of the Effect of Tissue Microstructure on Contraction in a Computational Model of Rat Left Ventricle. PLoS ONE, 2014, 9, e92792.	1.1	20
58	Interrogation of living myocardium in multiple static deformation states with diffusion tensor and diffusion spectrum imaging. Progress in Biophysics and Molecular Biology, 2014, 115, 213-225.	1.4	19
59	Three-dimensional histology: tools and application to quantitative assessment of cell-type distribution in rabbit heart. Europace, 2014, 16, iv86-iv95.	0.7	22
60	Images as drivers of progress in cardiac computational modelling. Progress in Biophysics and Molecular Biology, 2014, 115, 198-212.	1.4	47
61	Fractional diffusion models of cardiac electrical propagation: role of structural heterogeneity in dispersion of repolarization. Journal of the Royal Society Interface, 2014, 11, 20140352.	1.5	173
62	Bacterial cell identification in differential interference contrast microscopy images. BMC Bioinformatics, 2013, 14, 134.	1.2	23
63	Multiview diffeomorphic registration: Application to motion and strain estimation from 3D echocardiography. Medical Image Analysis, 2013, 17, 348-364.	7.0	17
64	Effect of Fibre Orientation Optimisation in an Electromechanical Model of Left Ventricular Contraction in Rat. Lecture Notes in Computer Science, 2013, , 46-53.	1.0	3
65	Modelling of the physiological response of the brain to ischaemic stroke. Interface Focus, 2013, 3, 20120079.	1.5	12
66	Model-Based Vasculature Extraction From Optical Fluorescence Cryomicrotome Images. IEEE Transactions on Medical Imaging, 2013, 32, 56-72.	5.4	30
67	Rearrangement of Atrial Bundle Architecture and Consequent Changes in Anisotropy of Conduction Constitute the 3-Dimensional Substrate for Atrial Fibrillation. Circulation: Arrhythmia and Electrophysiology, 2013, 6, 967-975.	2.1	67
68	Resolving the Three-Dimensional Histology of the Heart. Lecture Notes in Computer Science, 2012, , 2-16.	1.0	3
69	A bioimage informatics approach to automatically extract complex fungal networks. Bioinformatics, 2012, 28, 2374-2381.	1.8	42
70	Coherence enhancing diffusion filtering based on the Phase Congruency Tensor. , 2012, , .		5
71	Pulmonary lobe segmentation from CT images using fissureness, airways, vessels and multilevel B-splines. , 2012, , .		20
72	Local phase approaches to extract biomedical networks. , 2012, , .		0

5

#	Article	IF	CITATIONS
73	Contrast independent detection of branching points in network-like structures. Proceedings of SPIE, 2012, , .	0.8	7
74	Contrast-Independent Curvilinear Structure Detection in Biomedical Images. IEEE Transactions on Image Processing, 2012, 21, 2572-2581.	6.0	44
75	Multiview Fusion 3-d Echocardiography: Improving the Information and Quality of Real-Time 3-D Echocardiography. Ultrasound in Medicine and Biology, 2011, 37, 1056-1072.	0.7	40
76	Rabbit-specific ventricular model of cardiac electrophysiological function including specialized conduction system. Progress in Biophysics and Molecular Biology, 2011, 107, 90-100.	1.4	62
77	The evaluation of single-view and multi-view fusion 3D echocardiography using image-driven segmentation and tracking. Medical Image Analysis, 2011, 15, 514-528.	7.0	47
78	Modelling of pH dynamics in brain cells after stroke. Interface Focus, 2011, 1, 408-416.	1.5	44
79	On the Usage of GPUs for Efficient Motion Estimation in Medical Image Sequences. International Journal of Biomedical Imaging, 2011, 2011, 1-15.	3.0	4
80	The Systems Biology Approach to Drug Development: Application to Toxicity Assessment of Cardiac Drugs. Clinical Pharmacology and Therapeutics, 2010, 88, 130-134.	2.3	60
81	Development of an anatomically detailed MRI-derived rabbit ventricular model and assessment of its impact on simulations of electrophysiological function. American Journal of Physiology - Heart and Circulatory Physiology, 2010, 298, H699-H718.	1.5	192
82	Parallel Simulation for Parameter Estimation of Optical Tissue Properties. Lecture Notes in Computer Science, 2010, , 51-62.	1.0	4
83	Real-Time 3D Fusion Echocardiography. JACC: Cardiovascular Imaging, 2010, 3, 682-690.	2.3	31
84	Cardiac valve annulus manual segmentation using computer assisted visual feedback in three-dimensional image data. , 2010, 2010, 738-41.		4
85	Towards High-Resolution Cardiac Atlases: Ventricular Anatomy Descriptors for a Standardized Reference Frame. Lecture Notes in Computer Science, 2010, , 75-84.	1.0	1
86	Intramural spatial variation of optical tissue properties measured with fluorescence microsphere images of porcine cardiac tissue. , 2009, 2009, 1408-11.		8
87	Remodeling of the Connective Tissue Microarchitecture of the Lamina Cribrosa in Early Experimental Glaucoma. , 2009, 50, 681.		194
88	Local-phase based 3D boundary detection using monogenic signal and its application to real-time 3-D echocardiography images. , 2009, , .		45
89	Automatically Generated, Anatomically Accurate Meshes for Cardiac Electrophysiology Problems. IEEE Transactions on Biomedical Engineering, 2009, 56, 1318-1330.	2.5	124
90	Multiview RT3D Echocardiography Image Fusion. Lecture Notes in Computer Science, 2009, , 134-143.	1.0	25

#	Article	IF	CITATIONS
91	Ceneration of histo-anatomically representative models of the individual heart: tools and application. Philosophical Transactions Series A, Mathematical, Physical, and Engineering Sciences, 2009, 367, 2257-2292.	1.6	135
92	Relationship between structural changes and hyperpolarized gas magnetic resonance imaging in chronic obstructive pulmonary disease using computational simulations with realistic alveolar geometry. Philosophical Transactions Series A, Mathematical, Physical, and Engineering Sciences, 2009, 367, 2347-2369.	1.6	11
93	The Role of Blood Vessels in Rabbit Propagation Dynamics and Cardiac Arrhythmias. Lecture Notes in Computer Science, 2009, , 268-276.	1.0	11
94	Image-Driven Cardiac Left Ventricle Segmentation for the Evaluation of Multiview Fused Real-Time 3-Dimensional Echocardiography Images. Lecture Notes in Computer Science, 2009, 12, 893-900.	1.0	5
95	High Performance Computer Simulations of Cardiac Electrical Function Based on High Resolution MRI Datasets. Lecture Notes in Computer Science, 2008, , 571-580.	1.0	8
96	AN ITERATIVE METHOD FOR REGISTRATION OF HIGH-RESOLUTION CARDIAC HISTOANATOMICAL AND MRI IMAGES. , 2007, , .		5
97	Registration of Multiview Real-Time 3-D Echocardiographic Sequences. IEEE Transactions on Medical Imaging, 2007, 26, 1154-1165.	5.4	97
98	3D Visualization of Cardiac Anatomical MRI Data with Para-Cellular Resolution. Annual International Conference of the IEEE Engineering in Medicine and Biology Society, 2007, 2007, 147-51.	0.5	4
99	Abstract 1872: New Fusion Technique Significantly Improves Image Quality and Completeness of Datasets in Real Time 3 Dimensional Echocardiography. Circulation, 2007, 116, .	1.6	2
100	Segmentation of trabeculated structures using an anisotropic Markov random field: application to the study of the optic nerve head in glaucoma. IEEE Transactions on Medical Imaging, 2006, 25, 245-255.	5.4	37
101	Three-Dimensional Models of Individual Cardiac Histoanatomy: Tools and Challenges. Annals of the New York Academy of Sciences, 2006, 1080, 301-319.	1.8	89
102	Phase-Based Registration of Multi-view Real-Time Three-Dimensional Echocardiographic Sequences. Lecture Notes in Computer Science, 2006, 9, 612-619.	1.0	15
103	Adaptive Multiscale Ultrasound Compounding Using Phase Information. Lecture Notes in Computer Science, 2005, 8, 589-596.	1.0	31
104	Hierarchical image segmentation using a correspondence with a tree model. Pattern Recognition, 2004, 37, 47-59.	5.1	5
105	Improved Watershed Transform for Medical Image Segmentation Using Prior Information. IEEE Transactions on Medical Imaging, 2004, 23, 447-458.	5.4	594
106	Outlining of the prostate using snakes with shape restrictions based on the wavelet transform (Doctoral Thesis: Dissertation). Pattern Recognition, 1999, 32, 1767-1781.	5.1	75